

NRC Publications Archive Archives des publications du CNRC

OH/CH₂O/3-Pentanone PLIF applied to a stratified isooctane/air turbulent flame front

Vena, Patrizio; Deschamps, B.; Smallwood, Gregory; Johnson, M.

This publication could be one of several versions: author's original, accepted manuscript or the publisher's version. /
La version de cette publication peut être l'une des suivantes : la version prépublication de l'auteur, la version
acceptée du manuscrit ou la version de l'éditeur.

Publisher's version / Version de l'éditeur:

*Combustion Institute Canadian Section, 2008 Spring Technical Meeting
[Proceedings], 2008*

NRC Publications Archive Record / Notice des Archives des publications du CNRC :
<https://nrc-publications.canada.ca/eng/view/object/?id=c8d26d14-4564-45d5-bf68-9a869b908fe9>
<https://publications-cnrc.canada.ca/fra/voir/objet/?id=c8d26d14-4564-45d5-bf68-9a869b908fe9>

Access and use of this website and the material on it are subject to the Terms and Conditions set forth at
<https://nrc-publications.canada.ca/eng/copyright>

READ THESE TERMS AND CONDITIONS CAREFULLY BEFORE USING THIS WEBSITE.

L'accès à ce site Web et l'utilisation de son contenu sont assujettis aux conditions présentées dans le site
<https://publications-cnrc.canada.ca/fra/droits>

LISEZ CES CONDITIONS ATTENTIVEMENT AVANT D'UTILISER CE SITE WEB.

Questions? Contact the NRC Publications Archive team at
PublicationsArchive-ArchivesPublications@nrc-cnrc.gc.ca. If you wish to email the authors directly, please see the
first page of the publication for their contact information.

Vous avez des questions? Nous pouvons vous aider. Pour communiquer directement avec un auteur, consultez la
première page de la revue dans laquelle son article a été publié afin de trouver ses coordonnées. Si vous n'arrivez
pas à les repérer, communiquez avec nous à PublicationsArchive-ArchivesPublications@nrc-cnrc.gc.ca.

OH/CH₂O/3-Pentanone PLIF applied to a stratified isooctane/air turbulent flame front

P.C. Vena^a, B. Deschamps^a, G.J. Smallwood^b, M.R. Johnson^{a*}

^a *Mechanical and Aerospace Engineering, Carleton University, Ottawa, Canada*

^b *Combustion Group, Institute for Chemical Process & Environmental Tech., NRC*

1. Introduction

In next generation low emission/low fuel consumption devices such as gas turbines and direct injection engines, combustion occurs within a partially premixed turbulent regime. In such cases, idealized models for premixed and non-premixed combustion do not accurately depict flame front behaviour where variations in fuel concentration affect local flame structure, propagation velocity, wrinkling, thickness, flammability limits, and heat release. It is therefore necessary to build an experimental database in order to identify the effects of stratification on flame properties in a turbulent flow field.

Several recent studies have been performed on freely propagating flames [1-5], where the mixture is centrally ignited and propagates parallel to the mixture fraction. The majority of these studies focussed on increasing flammability limits. Although some results remain contradictory, it has been argued that heat and radicals from the burnt richer region feed the leaner region, and enhance its resistance to extinction. This is often referred to as “back support” or a “memory effect” [1-3] in that combustion, and more specifically the laminar flame speed, is not determined strictly by the reactant properties, but also by the composition and temperature of the burnt gas. Several other works have considered rod stabilized V-flames [6-10], where the leading branches propagate transversely to a gradient in mixture fraction, as is the case in the current study. The primary emphasis of these studies was to investigate dynamic properties of the flames including curvature, flame surface density, and heat release. Results have shown limited effects on curvature [6] whereas increased values in flame surface density have been observed. It has also been shown that the length scales of the mixture fraction have a significant effect on wrinkling and propagation velocity [4].

This paper describes an experimental investigation on partially premixed combustion through the use of a unique burner that enables variation of mixture fraction longitudinally along a flame, replicating conditions that are relevant to practical stratified combustion devices. A PLIF imaging setup that images OH, CH₂O, and 3-Pentanone has been implemented to correlate unburned mixture fraction, progress variable, and flame surface density in a stratified isooctane/air flame. Heat release measurements are also obtained from the pixel-by-pixel product of simultaneous OH and CH₂O images.

2. Experimental setup

A 65mm x 15mm rectangular exit burner was designed that permits controlled variation of the mixture fraction gradient for local equivalence ratios ranging from 0 to 2 along the long axis of the burner. The mixture fraction and mean flow velocity can be independently controlled using two pairs of fuel and air mass flow controllers. A more detailed description is provided in [11]. A partially premixed

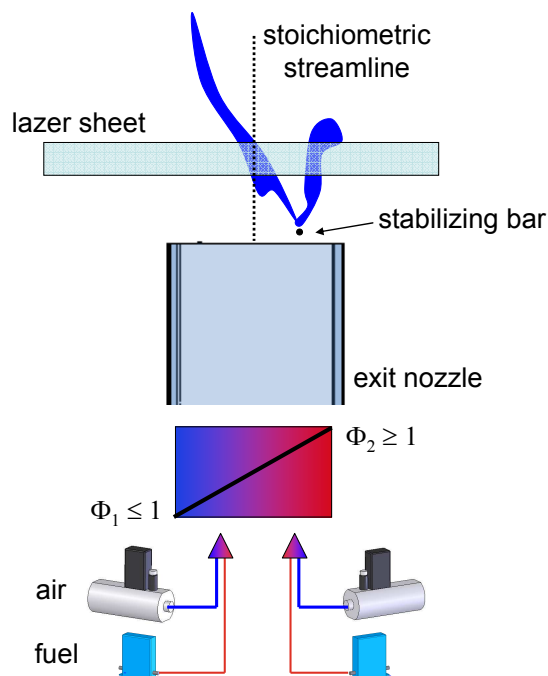


Figure 1. Stratified Burner with Laser Sheet

* Corresponding Author: Matthew_Johnson@carleton.ca

isooctane/air V-flame is stabilized with a 1.5 mm diameter rod placed perpendicularly to the exit nozzle of the burner. The stabilized partially premixed flame consists of two leading premixed branches and a trailing diffusion branch. The rod is positioned at $x=16.5$ mm from the inner edge on the rich side of the exit nozzle such that a continuous stratified flame front is present along the long axis of the rectangular burner, and the equivalence ratio along the flow centerline is approximately constant for all flame configurations (shown in Figure 1 as the stoichiometric streamline). Six flames were considered by increasing the equivalence ratio from 1 to 2 on the “rich” end of the burner, while decreasing from 1 to 0 on the lean end, in equivalence ratio steps of 0.2. For all tests, the average equivalence ratio over the burner exit plane was fixed at 1.0 and the mean flow velocity was fixed at 5 m/s.

OH/3-pentanone PLIF was performed using a Sirah Precision Scan Rhodamine B dye laser pumped by a frequency doubled Nd:YAG laser. Both were excited at 282nm (11mJ, 6ns) within a 15mm x 200 μ m laser sheet. Fluorescence images were captured by a 384x576 gated ICCD equipped with a Nikkor 105mm UV lens and UG 308nm HP filter to reject Raleigh scattering. Formaldehyde (CH₂O) PLIF images were recorded on a second 384x576 gated ICCD equipped with the same lens and a 355nm dichroic. A frequency tripled Quanta Ray YAG excites the CH₂O at 355nm (broadband, 7 ns) with a pulse energy of 300mJ and 3% standard deviation. Both laser sheets were collinear and pulses were monitored using a DG535 Stanford pulse generator to achieve the necessary pulse/gate synchronization and 200nsec delay between OH and CH₂O acquisitions. The PLIF images were recorded with a projected spatial resolution of 0.131 μ m/pixel, giving a good compromise between resolution, field of view imaging area, and laser sheet thickness. The laser diagnostic setup for simultaneous OH, CH₂O, and 3-pentanone PLIF, is presented in Figure 2.

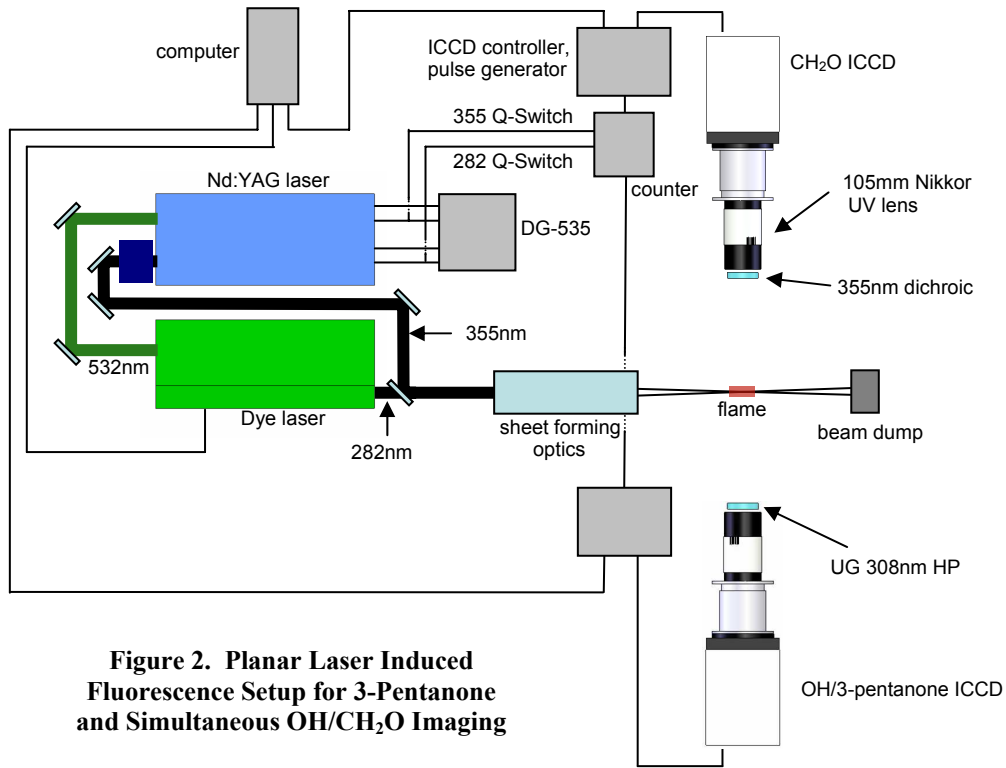


Figure 2. Planar Laser Induced Fluorescence Setup for 3-Pentanone and Simultaneous OH/CH₂O Imaging

3. Results and Discussion

The equivalence ratio gradient for each of the six flow settings under non-reacting conditions was characterised using 3-pentanone PLIF by seeding the isooctane with 3-pentanone at 4% by volume. One hundred individual images were acquired for each flame configuration. Images were then background corrected and cropped to only consider the most uniform region of the laser energy profile. Figures 3 a) and b) show the averaged homogeneous ($\phi \approx 1$) and stratified ($\Delta\phi \approx 0.032/\text{mm}$) cases used to obtain the profiles in 3 c) by summing the rows in these images. Figure 3 demonstrates the constant equivalence ratio along the stoichiometric streamline where all profiles intersect, which coincides with the center of the region of interest discussed in the following sections.

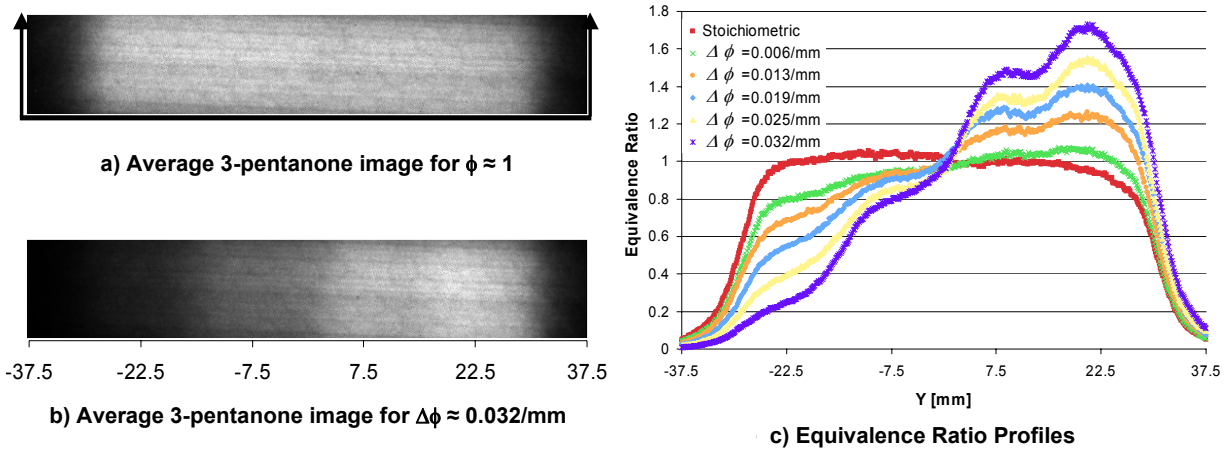


Figure 3. Equivalence Ratio Gradients for Six Flame Settings from 3-pentanone tracer PLIF

3.1 OH PLIF image description

300 images were acquired for each of the six flame configurations. Figure 4 shows typical single shot OH and CH_2O PLIF for each case along with the corresponding heat release map. The CH_2O images were first registered to the OH images using a 90 point target to spatially match each pixel of the OH and CH_2O images. This ensures the OH and CH_2O contours coincide and improves the accuracy of the heat release results. Images were then corrected for variations in background and laser energy profile before a threshold was applied.

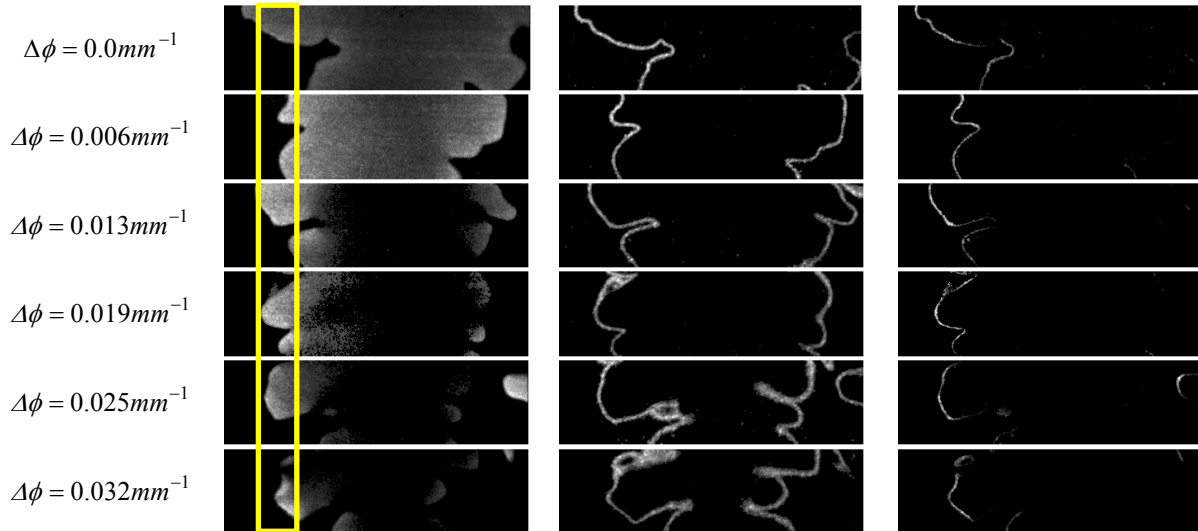


Figure 4. Instantaneous images of a) OH PLIF, b) CH_2O PLIF, and c) Heat Release

Figure 4a) compares a set of typical OH images for flames in varied mixture fraction gradients ranging from fully premixed to severely stratified. The OH radicals formed in the high temperature combustion zones are a marker for burnt gases and the “hot zone” in the flame front. In the homogeneous case, the OH appears throughout the burnt gases with higher fluorescence intensity near the boundary in areas of positive curvature, propagating towards the unburned mixture. It is suggested that this may be an indicator of higher heat release due to a strong production of OH radicals at high temperatures. It is also observed that the fluorescence intensity decreases away from the flame

front. In the homogeneous case, this is caused by lower temperatures present in the center of the flame. However, when a mixture gradient is applied to the flame front, OH concentrations seem to decrease more severely between premixed branches. This is more prominent as stratification increases.

Figure 5 shows average OH profiles across both flame fronts with the left premixed branch (the branch spanning the stoichiometric contour) identified with the outlined box. These profiles clearly show a drastic decrease in the amplitude of OH in the both flame branches, as the gradient in intensified as would be suggested by the more corrugated flame front for greater mixture gradients. This induces an increase in the flame surface density that can lead to local extinctions. Specific to the stratified flames, a weak diffusion flame occurs along the stoichiometric streamline which may also be enhanced by the presence of local extinctions in the premixed fronts.

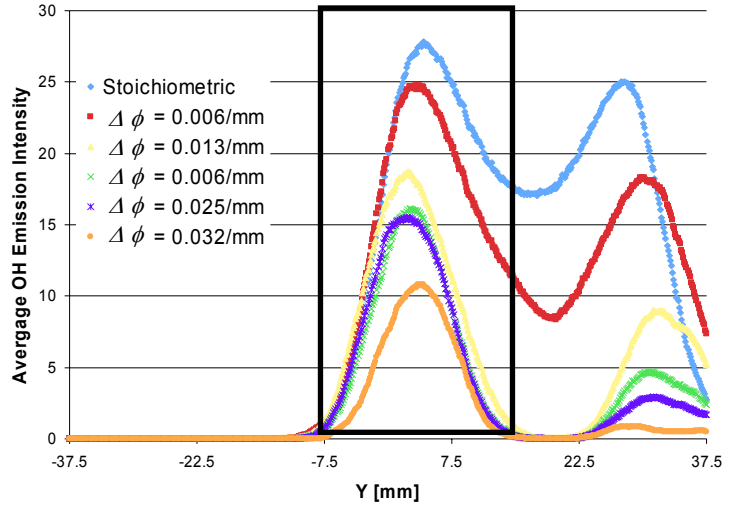


Figure 5. OH Profiles for Six Flame Settings

3.2 CH₂O PLIF and heat release image description

Figure 4b) confirms that formaldehyde generally follows the same outline as for OH PLIF. Formaldehyde is produced in the initial oxidation reaction i.e. at low temperatures in the early steps of hydrocarbon combustion and is therefore a marker of low temperature combustion zones and a good indicator of the cold limit of the flame front. Under stoichiometric conditions, the boundary of the flame front is very thin compared to that of the rich region as the thickness of the CH₂O front increases with local equivalence ratio. Figure 4b) also shows that the formaldehyde contours more closely match those of OH along the stoichiometric spanning front than the rich front, particularly in the homogeneous and mildly stratified cases. In fact, formaldehyde is destroyed to form HCO as it combines with OH radicals through $\text{CH}_2\text{O} + \text{OH} \rightarrow \text{HCO} + \text{H}_2\text{O}$ (A), a reaction that is a major contributor to heat release in the combustion process. On the branch spanning the stoichiometric contour, CH₂O meets excess OH radicals and rapidly combines to form HCO. Alternatively, on the rich branch, reaction (A) is not the major pathway for destroying CH₂O such that the OH and CH₂O fronts no longer match, making the OH x CH₂O product a less accurate marker of heat release in rich flames. The following discussion will consequently focus on the branch of the flame that spans the stoichiometric contour.

The outlined sections in Figure 4a) represent a 4mm wide region of interest (ROI) that is centered along the stoichiometric streamline, such that the equivalence ratio is assumed constant at $\phi \approx 1$. Within this window, it is observed that as the mixture gradient increases, the coincidence between OH and CH₂O fronts decreases, and the amount of CH₂O present outside the flame front increases. Specifically, the CH₂O becomes more diffuse for stronger gradients and suggests the presence of local extinctions, which are identified by regions of no heat release, or where OH and CH₂O are not both present. It is therefore proposed that a relation exists between the local heat release in 4c) and the amount of unbunrt CH₂O along the flame front. Further studies will attempt to correlate these two parameters by relating the local concentration of CH₂O to that of heat release.

In Figure 4c), maximum heat release is observed along the flame front at locations where OH fluorescence was highest, and seems unaffected by the increase in mixture gradient. The most significant change is observed in areas where CH₂O is diffuse and local heat release is very low. As the gradient increases, these low heat release areas tend to fade, and eventually disappear, suggesting flame extinction. These results suggest that the mixture fraction gradient decreases the minima of heat release along the flame front, but has limited effect on the maxima of heat release.

3.3 Flame Front Density and Heat Release

Flame surface density (FSD), defined here as the 2D flame front length divided by the flame front area, is obtained from processed OH PLIF images. A Frei-Chen gradient filter [12] is applied to each set of 300 individual images to obtain a map of the burnt gases. The results are averaged and the mean FSD is obtained for the previously discussed ROI for all six flames. Results are plotted in terms of the progress variable for cases where the ROI crossed the entire flame front and the progress variable ranged from 0 to 1.

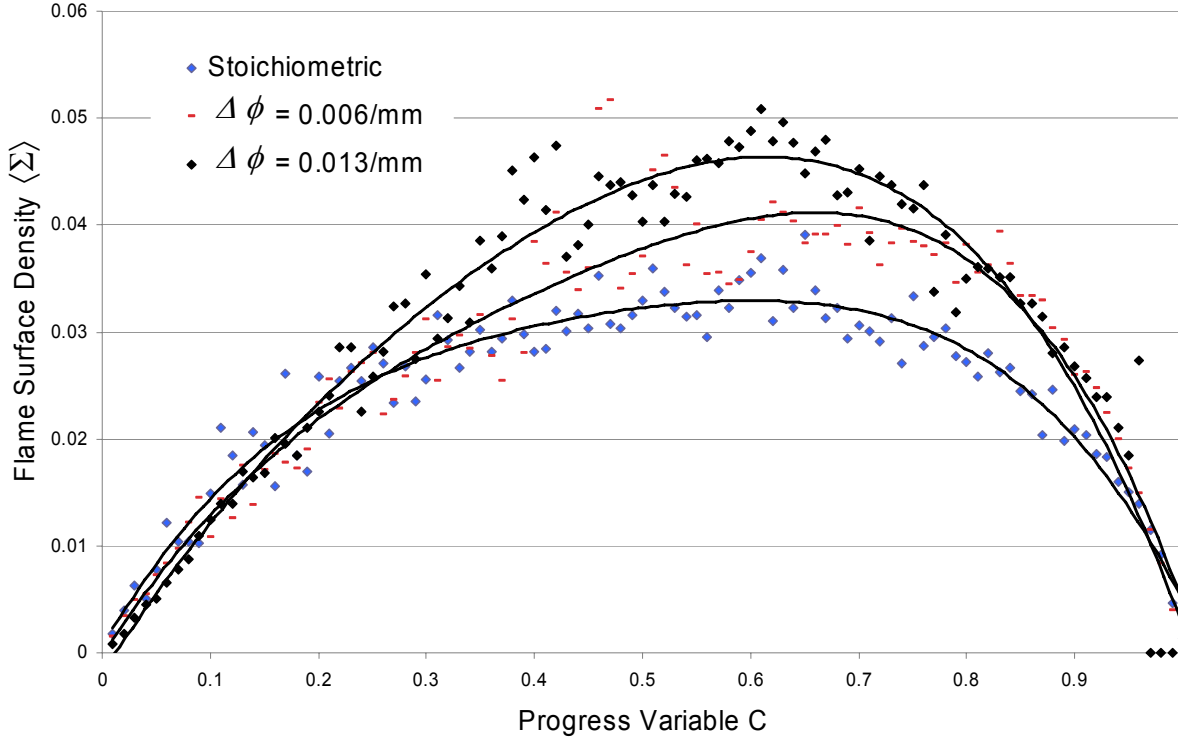


Figure 6. Flame Surface Density of OH for premixed and mildly stratified flames

Figure 6 shows skewed bell shaped curves for FSD with a maximum between 0.6 to 0.7. Results shows that FSD increases significantly with increasing mixture fraction. Results are in good agreement with those of Filho *et al.*[6] who studied globally lean ($\phi=0.73$) stratified turbulent methane/air V-flames. This result is further supported by the increased wrinkling that was observed for steeper gradients in the OH PLIF images. Figure 7 presents average heat release images of the stoichiometric branch and suggests a decrease in heat release as the mixture fraction increases.

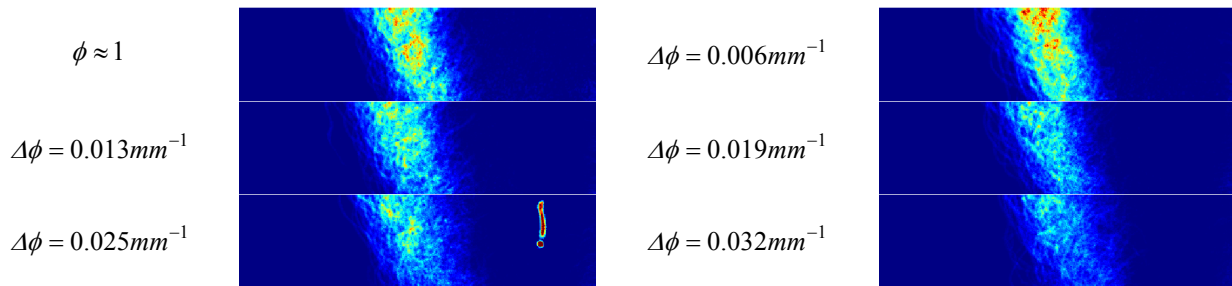


Figure 7. Mean Heat Release along Stoichiometric Branch

4. Conclusion

Six mixture fraction gradients have been applied to a globally stoichiometric isooctane-air flame front to study gradient effects on flame surface density and heat release. A PLIF imaging setup that images OH, CH₂O, and 3-Pentanone was implemented so that heat release could be measured from simultaneous OH and CH₂O images. It has been demonstrated that an increase in mixture fraction increases flame surface density for mildly stratified cases. In the present experiments, it was not possible to evaluate the effects of steeper gradients since the flame moved too far in the imaged PLIF interrogation window to permit accurate flame surface density measurements. The concentration of formaldehyde varies with gradient as instantaneous images show less and less coincidence between the OH and CH₂O contours, as well as the appearance of “blurred” CH₂O regions for stronger mixture fractions. Coupled with the heat release images, this suggests a relation between the regions of unburnt CH₂O and the presence of local extinctions along the flame front. It is hoped that this can further be correlated to heat release by associating local heat release to CH₂O concentrations.

REFERENCES

- [1] Y. Ra, W.K. Cheng, The Fifth International Symposium on Diagnostics and Modeling of Combustion in Internal Combustion Engines, 251-257, 2001.
- [2] A. Pires Da Cruz, A.M. Dean, J.M. Grenda, 28th Symp. (Int'l), The Comb. Inst., 1925-1932 (2000).
- [3] T. Kang, D.C. Kyritsis, Comb. Sci. and Tech., 177:2191-2210, 2005.
- [4] B. Renou, E. Samson, A. Boukhalfa, Comb. Sci. and Tech., 176:1864-1890, 2004.
- [5] N. Pasquier, *et al.*, 31st Symp. (Int'l), The Comb. Inst., 1567-1574 (2007)
- [6] P.A. Filho, C.N. Markedes, S. Hochgreb, Proceedings of the European Combustion Meeting (2007).
- [7] O. Degardin, PhD thesis, Institut National des Sciences Appliquées de Rouen, 2006.
- [8] O. Degardin, B. Renou, A. Boukhalfa, Exp in Fluids, 40:452-463, 2006.
- [9] D. Pave, PhD thesis, l'Université d'Orléans, 2002.
- [10] C. Galazzi, D. Escudie., Combustion and Flame, 145:621-634 (2006).
- [11] P.C. Vena, B. Deschamps, G.J. Smallwood, and M.R. Johnson, Proceedings of Combustion Institute Canadian Section Spring Technical Meeting, Waterloo, ON, paper G4-1 (2006).
- [12] O.L. Gulder *et al.*, Combustion and Flame, 120:407-416 (2000).